

Porous AlN films grown on C-face SiC by hydride vapor phase epitaxy

Jiafan Chen(陈家凡), Jun Huang(黄俊), Didi Li(李迪迪), and Ke Xu(徐科)

Citation: Chin. Phys. B, 2022, 31 (**7**): 076802. DOI: 10.1088/1674-1056/ac597e
Journal homepage: http://cpb.iphy.ac.cn; http://iopscience.iop.org/cpb

What follows is a list of articles you may be interested in

C_9N_4 as excellent dual electrocatalyst: A first principles study

Wei Xu(许伟), WenWu Xu(许文武), and Xiangmei Duan(段香梅)
Chin. Phys. B, 2021, 30 (**9**): 096802. DOI: 10.1088/1674-1056/ac0ccf

Preparation of AlN film grown on sputter-deposited and annealed AlN buffer layer via HVPE

Di-Di Li(李迪迪), Jing-Jing Chen(陈晶晶), Xu-Jun Su(苏旭军), Jun Huang(黄俊), Mu-Tong Niu(牛牧童), Jin-Tong Xu(许金通), and Ke Xu(徐科)
Chin. Phys. B, 2021, 30 (**3**): 036801. DOI: 10.1088/1674-1056/abd392

Full filling of mesoporous carbon nanotubes by aqueous solution at room temperature

Xiao-Na Ren(任晓娜), Min Xia(夏敏), Qing-Zhi Yan(燕青芝), Chang-Chun Ge(葛昌纯)
Chin. Phys. B, 2019, 28 (**3**): 036801. DOI: 10.1088/1674-1056/28/3/036801

Vibrational features of confined water in nanoporous TiO_2 by Raman spectra

Xin Gao(高欣), Qiang Wang(王强), Gang Sun(孙刚), Chen-Xi Li(李晨曦), Lin Hu(胡林)
Chin. Phys. B, 2016, 25 (**2**): 026801. DOI: 10.1088/1674-1056/25/2/026801

Effect of the thickness of InGaN interlayer on *a*-plane GaN epilayer

Wang Jian-Xia, Wang Lian-Shan, Zhang Qian, Meng Xiang-Yue, Yang Shao-Yan, Zhao Gui-Juan, Li Hui-Jie, Wei Hong-Yuan, Wang Zhan-Guo
Chin. Phys. B, 2015, 24 (**2**): 026802. DOI: 10.1088/1674-1056/24/2/026802

Porous AlN films grown on C-face SiC by hydride vapor phase epitaxy

Jiafan Chen(陈家凡), Jun Huang(黄俊)[†], Didi Li(李迪迪), and Ke Xu(徐科)[†]

Suzhou Institute of Nano-Tech and Nano-Bionics, Chinese Academy of Sciences, Suzhou 215123, *China*

(Received 19 October 2021; revised manuscript received 27 January 2022; accepted manuscript online 2 March 2022)

We report the growth of porous AlN films on C-face SiC substrates by hydride vapor phase epitaxy (HVPE). The influences of growth condition on surface morphology, residual strain and crystalline quality of AlN films have been investigated. With the increase of the V/III ratio, the growth mode of AlN grown on C-face 6H-SiC substrates changes from step-flow to pit-hole morphology. Atomic force microscopy (AFM), scanning electron microscopy (SEM) and Raman analysis show that cracks appear due to tensile stress in the films with the lowest V/III ratio and the highest V/III ratio with a thickness of about 3 μm. In contrast, under the medium V/III ratio growth condition, the porous film can be obtained. Even when the thickness of the porous AlN film is further increased to 8 μm, the film remains porous and crack-free, and the crystal quality is improved.

Keywords: hydride vapor phase epitaxy (HVPE), porous, AlN

PACS: 68.55.–a, 81.15.–z, 61.72.–y **DOI:** 10.1088/1674-1056/ac597e

1. Introduction

Porous nitride semiconductor is a rapidly developing research field.[1] It has opened up a series of new properties and applications including optical reflectors,[2] sensors,[3] catalysis,[4] as well as improving the material quality.[5] AlN has potential applications in power electronic and optoelectronic fields due to its wide bandgap, high breakdown voltages, high thermal conductivity and strong resistance to radiation. Hydride vapor phase epitaxy (HVPE) is expected to be promising for fabricating AlN thick films. Several researchers have attempted to grow AlN layers through HVPE by using SiC as a starting substrate for the preparation of AlN thick films, because SiC has good thermal conductivity and chemical stability for high-temperature application conditions, and the lattice and thermal expansion mismatches between AlN and SiC are low as well.[6–8]

However, due to the tensile strain of AlN grown on SiC substrate, the growth of thick and crack free films is very challenging. Without the use of stress control techniques, cracks are likely to occur when AlN films are thicker than 3 μm. In addition, AlN grown on SiC substrate would show rough surfaces due to the low migration length of adatoms.[9] The growth temperature and V/III ratio can affect the migration length of adatoms. Porous AlN film is an effective way to relax the strain in the AlN thick films. As for the HVPE method, however, the study of porous AlN thick films is less. Here, we demonstrated porous AlN films grown on C-face SiC by HVPE. The changes of surface morphology, crystal quality and stress state of AlN films with growth condition were studied. Finally, a porous AlN film with a maximum thickness of 8 μm and without cracks was grown.

2. Experiments

AlN films were grown on 2-in diameter *c*-oriented C-face 6H-SiC substrates by HVPE. The growth temperature was approximately 1400 °C and the growth pressure was 1 kPa. NH_3 and HCl were used as input active gases, a mixture of N_2 and H_2 served as carrier gas. $AlCl_3$ was formed by the reaction of Al and HCl at 550 °C in the source zone of the reactor for AlN growth. The growth conditions of AlN samples were shown in Table 1.

The surface and cross-sectional morphology of the samples was characterized by scanning electron microscopy (SEM) (FEI Quanta 250 FEG) and atomic force microscopy (AFM) (Veeco Dimension 3100). The Raman spectra were measured by using a LabRAM HR 800 spectrometer (HORIBA Scientific, Edison, NJ, USA), excited with a 532 nm laser. High-resolution x-ray diffraction (HR-XRD) measurements were performed on the x-ray diffractometer (Bruker D8 Discover). The microstructure observations were performed on a transmission electron microscope (Themis Z, USA) with an accelerating voltage of 300 kV. The cross-sectional specimens for TEM measurements were prepared by mechanical polishing and followed by the Ar^+ ion milling process.

3. Results and discussion

Figure 1 shows the top view SEM images of AlN samples S1–S4. The surface of sample S1 grown under V/III ratio of

[†]Corresponding author. E-mail: junhuang2008@sinano.ac.cn
[‡]Corresponding author. E-mail: kxu2006@sinano.ac.cn

© 2022 Chinese Physical Society and IOP Publishing Ltd

15 is smooth but with cracks as shown in Figs. 1(a) and 1(b). As the V/III ratio increases to 30, pits appear on the surface of the AlN film, as shown in Figs. 1(c) and 1(d), corresponding to sample S2. When the V/III ratio is further increased to 60, the surface uniformity of the AlN film deteriorates and cracks appear, as shown in Figs. 1(e) and 1(f), which correspond to sample S3. Figures 1(g) and 1(h) show the SEM image of sample S4. The growth conditions of sample S4 are as the same as sample 2, excepting that the thickness is increased from 3 μm to 8 μm. After increasing the thickness, the surface morphology of the AlN film still maintains a porous morphology, and there are no cracks. It is worth noting that the suitable V/III ratio could effectively suppress the cracks of samples.

Table 1. The growth conditions of AlN films.

Sample	Growth temperature (°C)	V/III ratio	Thickness (μm)
S1	1400	15/1	3
S2	1400	30/1	3
S3	1400	60/1	3
S4	1400	30/1	8

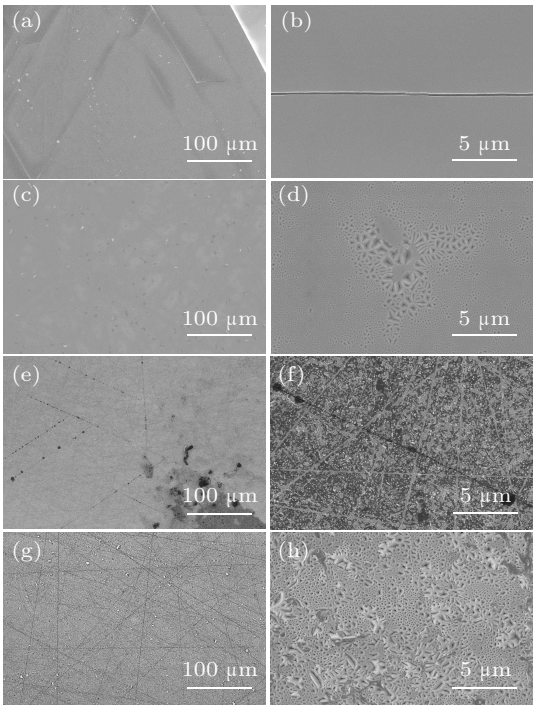


Fig. 1. Plan-view SEM images: (a) and (b) sample S1, (c) and (d) sample S2, (e) and (f) sample S3, (g) and (h) sample S4.

Figure 2 shows the AFM images over areas of 10 μm × 10 μm and 2 μm × 2 μm for the samples S1–S4, respectively. It is observed that the sample grown under a low V/III ratio of 15 exhibited a surface with step-flow morphology as shown in Figs. 2(a) and 2(b). The samples grown at V/III ratios of 30 and 60 all show porous surface morphology, as shown in Figs. 2(c)–2(f), and there are some cracks and some irregular island-like structures on the surface of the latter. Figure 1(d) shows the AFM image of sample S4. As the thickness increases, the AlN film still has a porous morphology, but the shape of the pores changes from polygonal to nearly circular. The density of the pores in sample S2, S3, and S4 is 8.45×10^9 cm^{-2}, 3.85×10^9 cm^{-2}, and 1.07×10^{10} cm^{-2}, respectively. It is speculated that the porous morphology could originate from the difficult coalescence during growth when the V/III is high. In another word, high V/III growth would deteriorate the surface morphology and make the coalescence growth of AlN film become more difficult.[10]

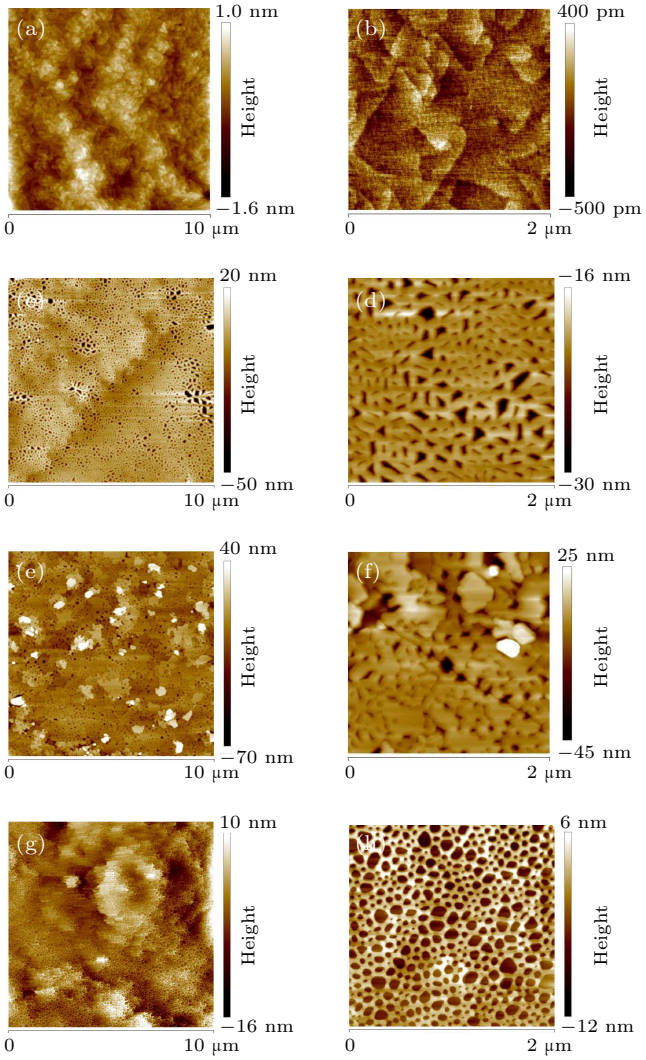


Fig. 2. AFM images of AlN films: (a) and (b) sample S1, (c) and (d) sample S2, (e) and (f) sample S3, (g) and (h) sample S4.

Figure 3 shows normalized Raman spectra of the E_2 (high) phonon mode for all the samples. The vertical line shows the stress-free frequency of 657.4 cm^{-1}.[6] The magnitude of each tensile stress is determined by the difference between its peak position and the stress free peak position. For biaxial stress can be estimated by

$$\sigma_{xx} = \Delta\omega_{E_2(\text{high})}/4.04. \quad (1)$$

The peak positions of the E_2 (high) phonon mode for samples S1–S4 are 651.99 cm^{-1}, 654.97 cm^{-1}, 652.74 cm^{-1}, and

654.25 cm^{-1}, corresponding to the biaxial tensile stress values of 1.34 GPa, 0.60 GPa, 1.15 GPa, and 0.78 GPa, respectively. The peaks for all samples appear on the lower frequency side of the stress-free position, showing their residual tensile stress. Samples S2 and S4 are under the low residual stress compared with samples S1 and S3, which indicates that the formation of porous AlN could relax the stress.

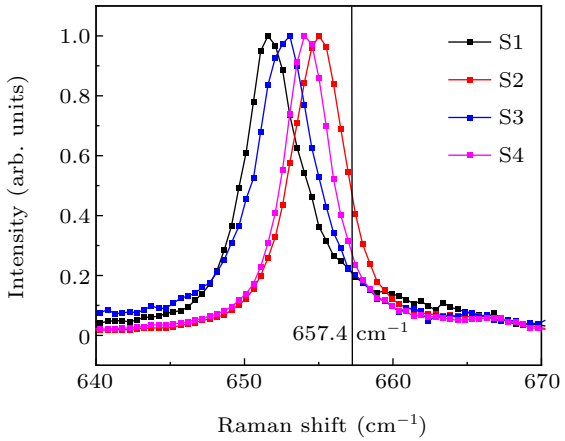


Fig. 3. Normalized Raman spectra of the AlN E_2 (high) phonon mode. The vertical line shows a stress-free frequency of 657.4 cm^{-1}.

Figure 4 shows the dependence of the full width at half maximum (FWHM) of the (0002) and (10-12)-plane x-ray rocking curves (XRCs) for samples S1–S3 on the V/III ratio. Threading dislocations in AlN films are associated with local lattice distortion. Screw-component and edge-component dislocations contribute to the broadening of the (0002) and (10-12) peak, respectively. The dislocation density of AlN films is evaluated by[11]

$$\rho_{\text{screw}} = \frac{\beta_{\text{tilt}}^2}{4.35 b_{\text{c}}^2}, \quad \rho_{\text{edge}} = \frac{\beta_{\text{twist}}^2}{4.35 b_{\text{a}}^2}, \tag{2}$$

where β_{tilt} and β_{twist} are the FWHMs of (0002) and (10-12) planes, b_{c} and b_{a} stand for the Burgers vectors of screw and edge threading dislocations, respectively. The FWHMs of the (0002) plane XRC for samples S1–S3 are 493 arcsec, 370 arcsec, 403 arcsec, corresponding to a density of screw-component TDs of about 5.29×10^8 cm^{-2}, 2.98×10^8 cm^{-2} and 3.53×10^8 cm^{-2}, respectively. The FWHMs of the (10-12) plane XRC for samples S1–S3 are 1004 arcsec, 810 arcsec, 986 arcsec, corresponding to a density of edge-component TDs of about 1.06×10^{10} cm^{-2}, 7.05×10^9 cm^{-2}, and 1.07×10^{10} cm^{-2}, respectively. The minimum FWHM of both the (0002) and (10-12)-plane XRC is obtained in the sample S2 with V/III ratio of 30, which is consistent with the Raman results where sample S2 has the lowest residual stress.

Figure 5 shows the (0002) and (1012)-plane x-ray rocking curves (XRCs) of samples S4. The FWHMs of the (0002) and (1012)-plane XRCs for sample S4 are 334 arcsec and 547 arcsec, corresponding to a density of screw-component and edge-component TDs of about 2.43×10^8 cm^{-2} and 2.89×10^9 cm^{-2}, respectively. Obviously, as the thickness increases, the crystal quality of the AlN film has been greatly improved.

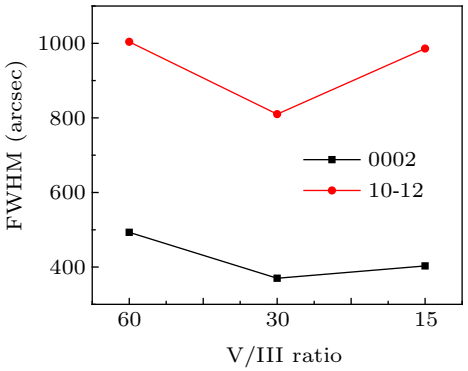


Fig. 4. The FWHM values of (0002) and (10-12) x-ray diffraction rocking curves of samples S1–S3.

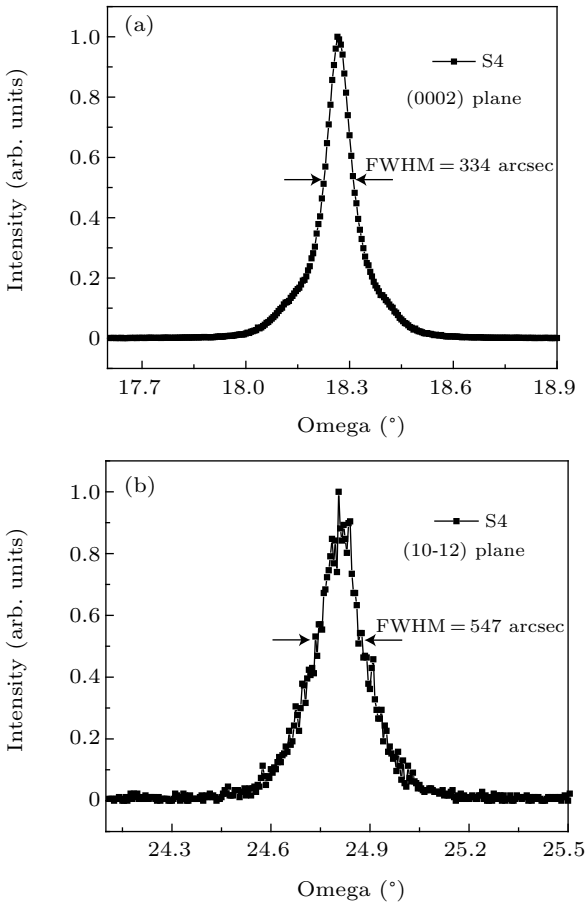


Fig. 5. The (0002) and (1012)-plane XRCs of sample S4.

Figure 6 shows cross-sectional SEM and TEM pictures of sample S4. It can be seen from the cross-sectional SEM and TEM that the pores on the surface of the AlN film are similar to V-shaped pits. Nanotubes attached to the bottom of the V-shaped pit. The structural characteristics and origin of these nanotubes require further investigation.

The strain energy of the film accumulates with the increase of film thickness and finally reaches a critical value to form cracks. The formation of cracks allows the strain energy

of the film to be converted into additional surface energy of the cracks, thereby reducing the free energy of the system. For porous AlN films, the existence of pores themselves are beneficial to relax strain energy, increasing the critical thickness for cracking. With the increase of film thickness, the crystal quality of AlN improves, which is a common phenomenon in III-nitride epitaxial films. This is because dislocations need to interact sufficiently within a certain thickness to combine or annihilate.

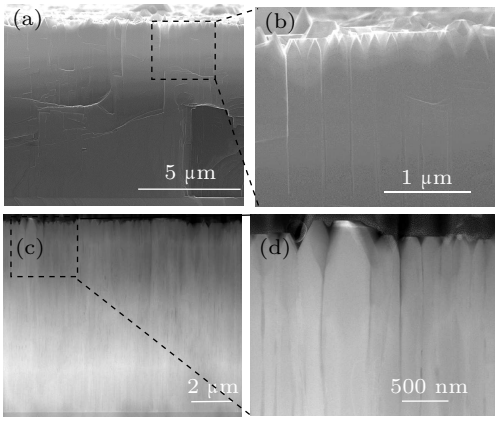


Fig. 6. (a) Cross-sectional SEM images of sample S4, (b) the magnified SEM images of the dashed rectangle in (a). (c) Cross-sectional TEM images of sample S4, (d) the magnified TEM images of the dashed rectangle in (c).

4. Conclusion

The influences of growth condition on surface morphology, residual strain and crystalline quality of AlN films have been investigated. Porous AlN films grown on C-face SiC by HVPE can be obtained on medium V/III. Porous AlN films can grow to 8 μm without cracks, and the crystal quality is improving with the increase of thickness. The characterization of cross-sectional SEM and TEM images show that the pores on the surface of aluminum nitride film are actually V-shaped pits. The bottom of each pit is connected with a microtubule penetrating the film. This discovery may have important value for the preparation and application of porous AlN materials.

References

[1] Griffin P H and Oliver R A 2020 *J. Phys. D* **53** 383002
[2] Zhang C, Park S H, Chen D, Lin D W, Xiong W, Kuo H C, Lin C F, Cao H and Han J 2015 *ACS Photon.* **2** 980
[3] Xi R, Zhang S H, Zhang L, Wang C, Wang L J, Yan J H and Pan G B 2019 *Sensors* **19** 606
[4] Cao D Z, Xiao H D, Xu H Z, Cui J S, Gao Q X and Pei H Y 2015 *Mater. Res. Bull.* **70** 881
[5] Bai J, Wang T, Parbrook P J and Cullis A G 2006 *Appl. Phys. Lett.* **89** 131925
[6] Chen J J, Su X J, Huang J, Niu M T and Xu K 2019 *J. Crys. Growth* **507** 196
[7] Lemettinen J, Okumura H, Kim I, Rudzinski M, Grzonka J and Palacios T 2018 *J. Crys. Growth* **487** 50
[8] Chen J J, Huang J, Su X J, Niu M T and Xu K 2020 *Chin. Phys. B* **29** 076802
[9] Lemettinen J, Okumura H, Kim I, Rudzinski M, Grzonka J, Palacios T and Suihkonen S 2018 *J. Crys. Growth* **487** 50
[10] Huang J, Chen Q J, Niu M T and Xu K 2020 *J. Cryst. Growth* **536** 125567
[11] Li D D, Chen J J, Su X J, Huang J, Niu M T, Xu J T and Xu K 2021 *Chin. Phys. B* **30** 036801